JACS
JOURNAL OF THE AMERICAN CHEMICAL SOCIETY
Article
pubs.acs.org/JACS

# Role of Loop-Clamping Side Chains in Catalysis by Triosephosphate Isomerase

Xiang Zhai, Tina L. Amyes, and John P. Richard*

Department of Chemistry, University at Buffalo, SUNY, Buffalo, New York 14260-3000, United States

Supporting Information

**ABSTRACT:** The side chains of Y208 and S211 from loop 7 of triosephosphate isomerase (TIM) form hydrogen bonds to backbone amides and carbonyls from loop 6 to stabilize the caged enzyme−substrate complex. The effect of seven mutations [Y208T, Y208S, Y208A, Y208F, S211G, S211A, Y208T/S211G] on the kinetic parameters for TIM catalyzed reactions of the whole substrates dihydroxyacetone phosphate and D-glyceraldehyde 3-phosphate [$(k_{cat}/K_m)_{GAP}$ and $(k_{cat}/K_m)_{DHAP}$] and of the substrate pieces glycolaldehyde and phosphite dianion $(k_{cat}/K_{HPi}K_{GA})$ are reported. The linear logarithmic correlation between these kinetic parameters, with slope of 1.04 ± 0.03, shows that most mutations of TIM result in an identical change in the activation barriers for the catalyzed reactions of whole substrate and substrate pieces, so that the transition states for these reactions are stabilized by similar interactions with the protein catalyst. The second linear logarithmic correlation [slope = 0.53 ± 0.16] between $k_{cat}$ for isomerization of GAP and $K_d^{\ddagger}$ for phosphite dianion binding to the transition state for wildtype and many mutant TIM-catalyzed reactions of substrate pieces shows that ca. 50% of the wildtype TIM dianion binding energy, eliminated by these mutations, is expressed at the wildtype Michaelis complex, and ca. 50% is only expressed at the wildtype transition state. Negative deviations from this correlation are observed when the mutation results in a decrease in enzyme reactivity at the catalytic site. The main effect of Y208T, Y208S, and Y208A mutations is to cause a reduction in the total intrinsic dianion binding energy, but the effect of Y208F extends to the catalytic site.

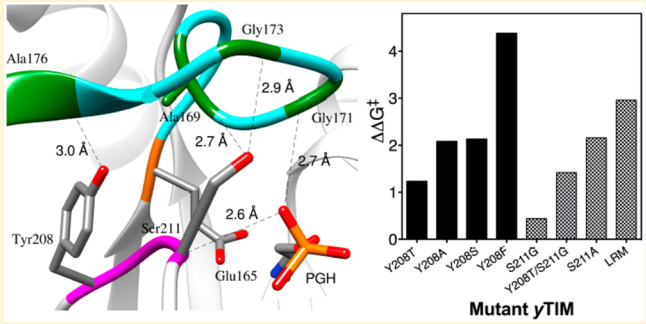


## INTRODUCTION

TIM catalyzes the conversion of dihydroxyacetone phosphate (DHAP) to (*R*)-glyceraldehyde 3-phosphate (GAP), by proton transfer reactions at carbon, through enzyme-bound *cis*-enediolate reaction intermediates (Scheme 1).[1−5] Classic studies by Knowles and co-workers focused on determination of the catalytic roles of the active site side chains, and were guided by the knowledge that similar mechanisms are observed for catalysis at enzyme active sites and in solution.[6,7] These studies showed that intramolecular proton transfer between C-1 and C-2 is performed by the carboxylate side-chain of Glu165,[8−12] while the neutral electrophilic imidazole side-chain of His-95 mediates proton transfer between O-1 and O-2 of the enediolate intermediate (Scheme 1).[13−15] The similarity in the mechanisms for nonenzymatic isomerization in water and isomerization at the active site of TIM was highlighted in a classic review entitled "*Enzyme catalysis: not different, just better*".[2]

We want to understand why the functional groups at the active site of TIM provide a greater stabilization of the transition state for deprotonation of carbon than the same groups in water.[4,16−18] This demands an explanation for the role of enzyme-phosphodianion interactions, which account for about 80% of the total transition state stabilization.[17,19] Knowles and associates identified the 11-residue phosphodianion gripper loop 6 [166-PVWAIGTGKTA] as an enabling structural element of TIM.[20,21] The binding of substrate DHAP[22] or transition state analogues phosphoglycolate (PGA)[23] and phosphoglycolohydroxamate (PGH)[24−26] to TIM triggers the closure of loop 6 over the ligand phosphodianion, and formation of *caged* enzyme-ligand complexes.[27] The deletion of residues 170−173 from loop 6 of TIM from chicken muscle (*c*TIM), and introduction of a peptide bond between A169 and K174 disrupts loop-dianion interactions. This results in a $10^5$-fold falloff in $k_{cat}/K_m$ for catalysis of isomerization due mainly to a decrease in $k_{cat}$,[20] so that the activating loop-dianion interactions develop only on moving from the ground-state Michaelis complex to the transition state for TIM-catalyzed isomerization.

Cutting the substrate for TIM into carbon acid and dianion pieces (Scheme 2) enables the enzyme-activating dianion interactions to be studied separately from anchoring interactions, which stabilize the Michaelis complex to the whole substrate. The strong activation of TIM-catalyzed deprotonation of glycolaldehyde by phosphite dianion ($HPO_3^{2-}$ = $HP_i$) shows that the TIM active site is divided into a catalytic domain, which contains the side chains that

**Received:** September 3, 2015
**Published:** November 16, 2015





DOI: 10.1021/jacs.5b09328
J. Am. Chem. Soc. 2015, 137, 15185−15197

**Scheme 1**

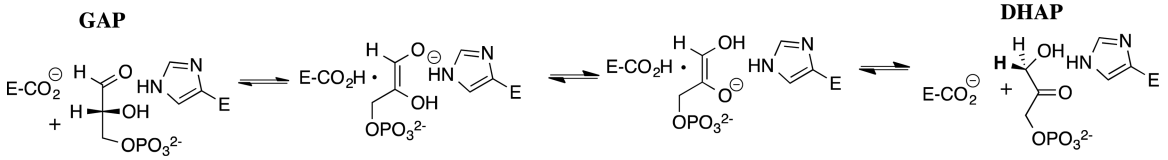


**Scheme 2**

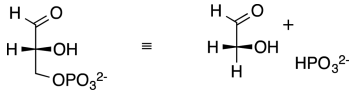

carry out chemical isomerization of bound substrate, and a dianion activation domain that uses enzyme-dianion interactions to promote the proton transfer reaction at the catalytic site.[28−30] The similar organization of the binding pockets of yeast orotidine 5′-monophosphate decarboxylase (*Sc*OMPDC)[30−33] and human L-glycerol 3-phosphate dehydrogenase (*hs*GPDH)[30,34,35] into catalytic and dianion activation domains is consistent with a common enzyme architecture that enables dianion activation of these and other protein catalysts.[36−38]

The activation of TIM, OMPDC, and GPDH for catalysis is achieved by sequestering their substrates at protein cages, which provide for optimal stabilizing interactions with the different reaction transition states.[27,39] Their active sites are formed through energetically demanding conformational changes,[40−42] in which the binding interactions between the protein and the substrate phosphodianion are used to *mold* flexible protein loops into caged structures.[4,12,22−29] Flexible loop 7 [208-YGGS-211] is part of the cage that activates TIM for catalysis of proton transfer. Closure of loop 6 is accompanied by 90° and 180° rotations, respectively, in the planes defined by the peptide bonds of G209 and G210 from loop 7. This swings the $-CH_2OH$ of S211 into position to hydrogen bond with the backbone carbonyl oxygen and amide nitrogen from A169 and G173, respectively; and, the S211 backbone amide NH group into a position to hydrogen bond with the ligand dianion.[5,42−44] An additional hydrogen bond forms between the side chain of Y208 and the backbone amide nitrogen from A176.[5,42,44]

Knowles and Sampson noticed these "*new hydrogen bonds between the hydroxyl groups of tyrosine-208 and serine-211*",[44] and characterized the kinetic parameters for Y208F and S211A mutants of yeast TIM (*y*TIM). The large falloff in the activity observed for these mutant enzymes was interesting, because the 8−9 Å separation between Y208 and S211 and the substrate (Figure 1) allows for minimal direct interactions with the isomerization transition state. Knowles and Sampson proposed that this falloff in activity reflects destabilization of the active closed form of TIM with respect to the open enzyme.[44] We have used our experimental protocol for the study of TIM-catalyzed reactions to probe the effects of site-directed mutations on the activity of TIM.[12,45−51] We report here the results of experiments that were designed to address the following questions:

(1) Is it possible to localize the effects of mutations at loop 7 to the loss of a single hydrogen-bonding interaction? The dienolate intermediate of the reaction catalyzed by bacterial ketosteroid isomerase (KSI) is stabilized by a hydrogen bond to the phenol side chain of Y16.[52] The 5000-fold falloff in activity

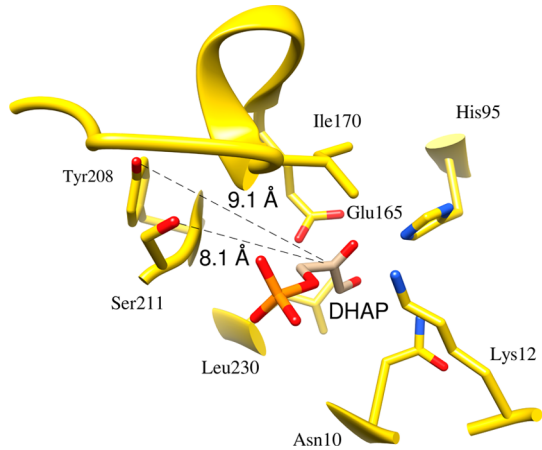


**Figure 1.** Representation of TIM, which shows the distance between loop 7 side chains Y208 and S211 at the dianion activation site, and the bound substrate DHAP at the catalytic site (PDB entry 1NEY]. The 8−9 Å separation between Y208 and S211 and the substrate allows for minimal direct interactions with the isomerization reaction transition state.

of the Y16F mutant of KSI from *Pseudomonas putida* is ca. 100-fold larger than that for Y16A, Y16G, Y16S, and Y16T mutants, so that large effect of the Y16F mutation on enzyme activity is not due only to the loss of a single hydrogen bond.[53,54] We have prepared Y208F, Y208T, Y208S, and Y208A mutants of TIM, and determined kinetic parameters that are up to 200-fold greater than that for Y208F. We also find that the activity of S211G TIM is 20-fold greater than that for the S211A TIM.[44] We conclude that the loss of hydrogen bonds to altered Y208 and S211 side chains is no more than partly responsible for these changes in enzyme activity.

(2) What is the role of Y208 and S211 side chains from loop 7 in phosphite dianion activation of *y*TIM for catalysis of deprotonation of glycolaldehyde? The large 9.1 and 8.1 Å (Figure 1) distance, respectively, between the side chains of Y208 and S211 and C-2 of bound DHAP prevents direct interactions with the enzyme-bound ligand. The observed effects of these mutations on the enzyme kinetic parameters must therefore reflect effects that arise from changes in the structure of the active site cage. Our results suggest that the hydrogen bond to Y208 fixes the hydrophobic phenyl group over the active site cage, so as to minimize the local dielectric constant and optimize electrostatic and H-bonding interactions between TIM and bound phosphite dianion.

(3) What is the role, if any, for protein dynamics in the process of enzyme activation by phosphite dianion? Transition state theory provides a powerful framework for describing the activation barriers to enzyme-catalyzed reactions determined by kinetic analyses, and in rationalizing the changes in these activation barriers for mutant enzymes. We report that a two-state model that defines the activation barrier $\Delta G^{\ddagger}$ for TIM-catalyzed reactions as the difference in energy of the free


DOI: 10.1021/jacs.5b09328
J. Am. Chem. Soc. 2015, 137, 15185−15197

reactants and enzyme-bound transition state provides a satisfactory rationalization of these results. Our results do not rigorously exclude effects that arise from changes in protein dynamics, but sets conditions on models for these dynamic effects.

An earlier communication reported that five mutations of Y208, S211 yeast TIM and of other side chains of TIM from several organisms result in nearly the same change in the activation barriers for the catalyzed reactions of whole substrate and substrate pieces.[28] We concluded that that the two transition states are stabilized by essentially the same interactions with the protein catalyst. We report here the full results from studies on a total of seven mutants of Y208, S211, and an internally consistent rationalization for their effect on the catalytic activity of TIM.

## EXPERIMENTAL PROCEDURES

**Materials.** Dihydroxyacetone phosphate (magnesium salt), NADH (disodium salt), Dowex 50WX4-200R, triethanolamine hydrochloride (TEA·HCl), dithiothreitol (DTT), rabbit muscle glycerol 3-phosphate dehydrogenase, and glyceraldehyde 3-phosphate dehydrogenase were purchased from Sigma. $NAD^+$ (free acid) was purchased from MP Biomedical. Bovine serum albumin was purchased from Roche. DEAE Sepharose Fast Flow was purchased from GE Healthcare. Hydrogen arsenate heptahydrate and sodium phosphite (dibasic, pentahydrate) were purchased from Fluka. Sodium phosphite was dried under vacuum as described in earlier work.[16] [1-$^{13}$C]-Glycolaldehyde (99% enrichment of $^{13}$C at C-1, 0.09 M in water) was purchased from Omicron Biochemicals. Deuterium oxide (99% D) and deuterium chloride (35% w/w, 99.9% D) were purchased from Cambridge Isotope Laboratories. Imidazole was recrystallized from benzene. All other chemicals were reagent grade or better and were used without further purification. The disodium salt of D-glyceraldehyde 3-phosphate diethyl acetal was prepared by a literature procedure,[55] and purified by column chromatography over DEAE-Sephadex. Stock solutions of D-glyceraldehyde 3-phosphate (GAP) were prepared by hydrolysis of the corresponding diethyl acetal using Dowex 50WX4-200R ($H^+$ form) in boiling $H_2O$.[46] The resulting solutions were stored at −20 °C and adjusted to pH 7.5 by the addition of 1 M NaOH prior to use in enzyme assays. Stock solutions of phosphite dianion and [1-$^{13}$C]-glycolaldehyde ([1-$^{13}$C]-GA) in $D_2O$ were prepared as described in earlier work.[16,47]

**Preparation of Enzymes.** The plasmid containing the gene for wildtype TIM from *Saccharomyces cerevisiae* was a generous gift from Professor Nicole Sampson.[47] The procedures for site-direct mutagenesis used to introduce Y208A, Y208T, Y208S, Y208F, and S211A mutations are described in the Supporting Information to ref 28. The plasmids for the single S211G and the double Y208T/S211G mutants were prepared by introducing the S211G mutation onto the wildtype or Y208T-encoding template using the primers 5′-C-GAA-TTG-AGA-ATC-TTA-TAC-GGT-GGT-GGC-GCT-AAC-GGT-AGC-AAC-GC-3′ and 5′-GC-GAA-TTG-AGA-ATC-TTA-ACC-GGT-GGT-GGC-GCT-AAC-GGT-AGC-AAC-GCC-3′, respectively. Following amplification by PCR, the methylated parent DNA was treated with 20 units of the restriction enzyme *Dpn*I at 37 °C for 1 h, and then transformed into the *Escherichia coli* strain K802. Plasmid DNA samples from several colonies were purified using the QIAprep Miniprep Kit from Qiagen. The DNA sequence of the genes for the S211G and Y208T/S211G mutants was verified by sequencing at the Roswell Park Cancer Institute (Buffalo, NY).

Wildtype and mutant *y*TIMs were expressed using the TIM-deficient *tpi*A$^-$ lDE3 lysogenic strain of *E. coli*, FB215471(DE3)[30] grown in LB medium at 37 °C. The enzymes were purified by DEAE Sepharose column chromatography after fractional purification by polyethylenimine (0.33%) and ammonium sulfate precipitation.[56] These proteins were judged to be homogeneous by gel electrophoresis. Enzyme concentrations were determined based upon their absorbance at 280 nm using the extinction coefficients of 25440 $M^{-1}cm^{-1}$ for wildtype and S211 mutants and 23950 $M^{-1}cm^{-1}$ for Y208 mutants, calculated by the ProtParam tool available on the Expasy server.[57,58]

**Enzyme Assays.** All enzyme solutions were exhaustively dialyzed against 20 mM triethanolamine buffer (pH 7.5) at 7 °C prior to use; and the enzyme assays were carried out in the same buffer at 25 °C and $I$ = 0.1 (NaCl). D-Glycerol 3-phosphate dehydrogenase was assayed by monitoring the oxidation of NADH by DHAP; and glyceraldehyde 3-phosphate dehydrogenase was assayed by monitoring the enzyme-catalyzed reduction of $NAD^+$ by GAP.

The TIM-catalyzed isomerization of GAP was monitored by coupling the formation of the product DHAP to the oxidation of NADH catalyzed by L-glycerol 3-phosphate dehydrogenase.[46,47] The TIM-catalyzed isomerization of DHAP was monitored by coupling the formation of the product GAP to the reduction of $NAD^+$ catalyzed by glyceraldehyde 3-phosphate dehydrogenase in the presence of 2−10 mM arsenate.[50,59] The values of $k_{cat}$ and $K_m$ for mutant *y*TIM-catalyzed isomerization of GAP or DHAP were determined from the fit to the Michaelis−Menten equation of initial velocities ($v_i$) determined at varying concentrations of substrate. Values for $k_{cat}$, $K_m$, and $K_i$ for mutant *y*TIM-catalyzed reaction of DHAP were determined from the nonlinear least-squares fit to eq 1 of initial velocities determined at varying concentrations of arsenate dianion and DHAP.

$$\frac{v_i}{[E]} = \frac{k_{cat}[DHAP]}{K_m(1 + [HOAsO_3^{2-}]/K_i) + [DHAP]} \quad (1)$$

**$^1$H NMR Analyses.** $^1$H NMR spectra at 500 MHz were recorded in $D_2O$ at 25 °C using a Varian Unity Inova 500 spectrometer that was shimmed to give a line width of ≤0.5 Hz for the most downfield peak of the double triplet due to the C-1 proton of the hydrate of [1-$^{13}$C]-GA.[47] Spectra (16−64 transients) were obtained using a sweep width of 6000 Hz, a pulse angle of 90° and an acquisition time of 6 s. A total relaxation delay of 120 s (>8$T_1$) between transients was used to ensure that accurate integrals were obtained for the protons of interest.[60,61] Baselines were subjected to a first-order drift correction before determination of integrated peak areas. Chemical shifts are reported relative to that for HOD at 4.67 ppm.

**TIM-Catalyzed Reactions of [1-$^{13}$C]-GA in $D_2O$ Monitored by $^1$H NMR.** The mutant *y*TIM-catalyzed reactions of [1-$^{13}$C]-GA in the presence or absence of $HPO_3^{2-}$ in $D_2O$ at 25 °C were monitored by $^1$H NMR analyses as described in earlier work.[47,62] The enzyme was first exhaustively dialyzed at 7 °C against 30 mM imidazole (20% free base, pD 7.0) in $D_2O$ ($I$ = 0.024 or 0.1 (NaCl)). The reactions in the absence of phosphite dianion were initiated by adding enzyme to give a final solution that contained 20 mM [1-$^{13}$C]-GA, 20 mM imidazole (20% free base, pD 7.0, $I$ = 0.1 (NaCl)), and enzyme [0.40 mM, wildtype *y*TIM; 0.10 mM, Y208T *y*TIM; 0.058 mM, Y208S *y*TIM; 0.068 mM, Y208A *y*TIM; 0.24 mM, Y208F *y*TIM; 0.47 mM, S211A *y*TIM; 0.26 mM, S211G *y*TIM; 0.18 mM, Y208T/S211G *y*TIM] in a volume of 850 μL. The reactions in the presence of $HPO_3^{2-}$ were initiated by adding enzyme to give a final solution that contained 20 mM [1-$^{13}$C]-GA, 20 mM imidazole (20% free base, pD 7.0), 1−40 mM $HPO_3^{2-}$ (50% dianion, pD 7.0), and enzyme [18−27 μM, wildtype *y*TIM; 20−61 μM, Y208T *y*TIM; 28−44 μM, Y208S *y*TIM; 41−61 μM, Y208A *y*TIM; 130−260 μM, Y208F *y*TIM; 50−370 μM, S211A *y*TIM; 11−38 μM, S211G *y*TIM; 25−68 μM, Y208T/S211G *y*TIM] in a volume of 850 μL ($I$ = 0.1, NaCl). In every case, 750 μL of the reaction mixture was transferred to an NMR tube, the $^1$H NMR spectrum was recorded immediately, and spectra were then recorded at regular intervals. The remaining solution was incubated at 25 °C and the activity of TIM for catalysis of isomerization of GAP monitored. No significant loss in activity of TIM was observed during any of these reactions. At the end of each NMR experiment, the protein was removed by ultrafiltration and the solution pD was determined. There was no significant change in pD during any of these reactions.

The observed $^1$H NMR peak areas for the reaction products were normalized, as described in previous work.[47] The fraction of the


DOI: 10.1021/jacs.5b09328
J. Am. Chem. Soc. 2015, 137, 15185−15197

**Table 1. Kinetic Parameters for Isomerization of GAP and DHAP Catalyzed by Wildtype and Mutant Forms of Triosephosphate Isomerase from Yeast at pH 7.5 and 25 °C[a]**

| | GAP[b] | | | DHAP[c] | | | |
|---|---|---|---|---|---|---|---|
| TIM | $k_{cat}$ ($s^{-1}$) | $K_m$ (mM) | $k_{cat}/K_m$ ($M^{-1}$ $s^{-1}$)[d] | $k_{cat}$ ($s^{-1}$) | $K_m$ (mM) | $k_{cat}/K_m$ ($M^{-1}$ $s^{-1}$) | $K_i$ (mM)[e] arsenate |
| wildtype | 8900 ± 700 | 1.0 ± 0.1 | (8.9 ± 1.1) × $10^6$<br>2.2 × $10^8$ | 860 ± 10 | 1.7 ± 0.1 | (5.1 ± 0.3) × $10^5$ | 6.5 ± 0.7 |
| Y208T | 3700 ± 50 | 3.4 ± 0.1 | (1.1 ± 0.1) × $10^6$<br>2.8 × $10^7$ | 580 ± 10 | 11 ± 1 | (5.3 ± 0.5) × $10^4$ | >25 |
| Y208S | 940 ± 30 | 3.9 ± 0.2 | (2.4 ± 0.1) × $10^5$<br>6.0 × $10^6$ | 250 ± 5 | 25 ± 3 | (1.0 ± 0.1) × $10^4$ | >25 |
| Y208A | 740 ± 10 | 2.9 ± 0.1 | (2.6 ± 0.1) × $10^5$<br>6.5 × $10^6$ | 210 ± 5 | 17 ± 1 | (1.2 ± 0.1) × $10^4$ | >25 |
| Y208F | 13 ± 1 | 2.4 ± 0.1 | (5.4 ± 0.5) × $10^3$<br>1.4 × $10^5$ | 4.5 ± 0.3 | 17 ± 2 | 260 ± 40 | ≥25 |
| S211A | 2800 ± 100 | 12 ± 0.1 | (2.3 ± 0.7) × $10^5$<br>5.8 × $10^6$ | linear plot | | (1.0 ± 0.3) × $10^4$ | >25 |
| S211G | 7500 ± 500 | 1.8 ± 0.3 | (4.2 ± 0.8) × $10^6$<br>1.05 × $10^8$ | 810 ± 10 | 3.2 ± 0.1 | (2.5 ± 0.4) × $10^5$ | 14 ± 1 |
| Y208T/S211G | 520 ± 30 | 0.71 ± 0.05 | (7.3 ± 0.8) × $10^5$<br>1.8 × $10^7$ | 135 ± 5 | 4.0 ± 0.2 | (3.4 ± 0.2) × $10^4$ | 18 ± 2 |
| 208-TGAG for 208-YGGS (LRM)[f] | 16 | 0.27 | 5.9 × $10^4$<br>1.5 × $10^5$ | 8.0 | 4.0 | 2.0 × $10^3$ | 3.8 |

[a]Under standard assay conditions of 30 mM triethanolamine buffer at pH 7.5, 25 °C and $I$ = 0.1 (NaCl). The kinetic parameters have been calculated using the total concentration of GAP or DHAP, unless indicated otherwise. [b]The errors for TIM-catalyzed isomerization of GAP were determined from the average of kinetic parameters determined in three separate experiments. [c]The errors for TIM-catalyzed isomerization of DHAP are the standard deviations determined from the nonlinear least-squares fits of the kinetic data. [d]The upper value is calculated for the total concentration of substrate GAP, and the lower is calculated for the reactive carbonyl form, which is 4% of total GAP. [e]The initial velocity of the isomerization of several concentrations of DHAP was determined in the presence of 2, 5, and 10 mM arsenate. [f]Loop replacement mutation of TIM from chicken muscle [ref 29].

**Scheme 3**

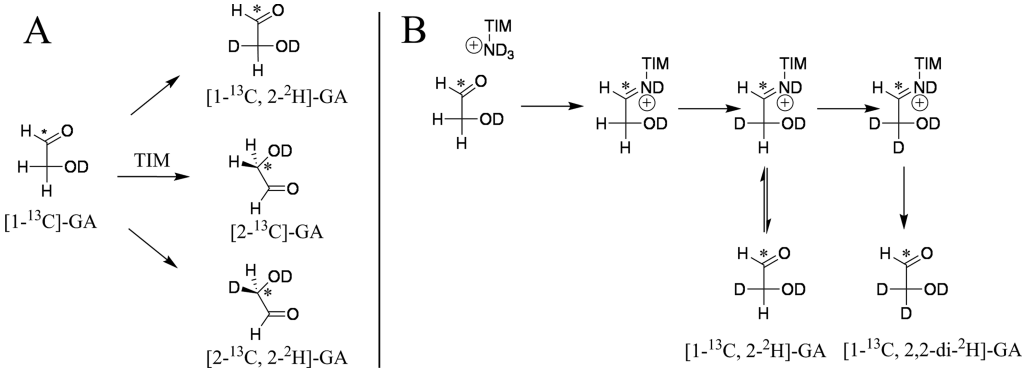


substrate [1-$^{13}$C]-GA remaining and the fractional yields of the identifiable reaction products [2-$^{13}$C]-GA, [2-$^{13}$C, 2-$^{2}$H]-GA, [1-$^{13}$C, 2-$^{2}$H]-GA, and [1-$^{13}$C, 2,2-di-$^{2}$H]-GA were determined from the integrated areas of the relevant $^{1}$H NMR signals for these compounds.[47] The disappearance of 30−70% [1-$^{13}$C]-GA was monitored, and product yields were determined over the first ca. 20−30% of the reaction. Observed first-order rate constants, $k_{obs}$ ($s^{-1}$), for the reactions of [1-$^{13}$C]-GA were determined from the slopes of linear semilogarithmic plots of reaction progress against time (eq 2), where $f_S$ is the fraction of [1-$^{13}$C]-GA remaining at time $t$. Observed second-order rate constants, $(k_{cat}/K_m)_{obs}$ ($M^{-1}$ $s^{-1}$), for the TIM-catalyzed reaction of [1-$^{13}$C]-GA were determined from the values of $k_{obs}$ using eq 3, where $f_{hyd}$ = 0.94 is the fraction of [1-$^{13}$C]-GA present as the hydrate.[16]

$$\ln f_S = -k_{obs}t \quad (2)$$

$$(k_{cat}/K_m)_{obs} = \frac{k_{obs}}{(1 - f_{hyd})[TIM]} \quad (3)$$

## RESULTS

The kinetic parameters for the isomerization reactions of GAP and DHAP catalyzed by wildtype and Y208 and S211 mutants of *y*TIM, determined at pH 7.5 and 25 °C ($I$ = 0.1, NaCl), are reported in Table 1. The kinetic parameters for the 208-TGAG for 208-YGGS loop 7 replacement mutation (LRM) at TIM from chicken muscle (Table 1) were determined in earlier work.[29] Arsenate is a required activator of glyceraldehyde 3-phosphate dehydrogenase, the coupling enzyme in assays of TIM-catalyzed isomerization of DHAP. Table 1 also reports the values of $K_i$ for arsenate inhibition of the mutant TIM-catalyzed reactions. The values of $k_{cat}/K_m$ reported in Table 1 were


DOI: 10.1021/jacs.5b09328
J. Am. Chem. Soc. 2015, 137, 15185−15197

**Table 2. Kinetic Parameters (Scheme 4) for the Unactivated and the Phosphite Dianion-Activated Reactions of the Carbonyl Form of [1-$^{13}$C]-GA Catalyzed by Wildtype and Mutant Variants of *y*TIM in $D_2O$ at 25 °C[a]**

| *y*TIM | $(k_{cat}/K_m)_E$ ($M^{-1}$ $s^{-1}$)[b] | $(k_{cat}/K_m)_{E•HPi}$ ($M^{-1}$ $s^{-1}$)[c] | $K_d$ (mM)[d] | $K_d^{‡}$ (mM)[e] | ΔG‡ (kcal/mol)[f] | $(k_{cat}/K_m)_{E•HPi}/K_d$ ($M^{-2}$ $s^{-1}$)[g] |
|---|---|---|---|---|---|---|
| wildtype | 0.062 | 48 ± 4 | 18 ± 3 | 0.023 | −6.3 | 2700 ± 500 |
| Y208T | 0.065 | ≈21 | ≈47 | 0.17 | −5.1 | 390 ± 3 |
| Y208S | 0.071 | ≈4.3 | ≈46 | 0.91 | −4.1 | 78 ± 6 |
| Y208A | 0.050 | linear plot | | 0.79 | −4.2 | 63 ± 3 |
| Y208F | 0.003 | linear plot | | 1.4 | −3.9 | 2.1 ± 0.1 |
| S211G | 0.13 | ≈210 | ≈63 | 0.048 | −5.9 | 2900 ± 200 |
| S211A | 0.002 | linear plot | | 0.025 | −6.3 | 79 ± 2 |
| Y208T/S211G | 0.12 | 18 ± 4 | 28 ± 3 | 0.20 | −5.0 | 600 ± 100 |
| 208-TGAG for 208-YGGS (LRM)[h] | 0.0045 | 0.39 | 4.1 | 0.048 | −5.9 | 95 |

[a]Determined by $^1$H NMR analysis of the products of the reaction of 20 mM [1-$^{13}$C]-GA in $D_2O$ at pD 7.0 (20 mM imidazole), 25 °C and $I$ = 0.1 (NaCl). [b]Second-order rate constant for the unactivated TIM-catalyzed reaction of [1-$^{13}$C]-GA in the absence of phosphite dianion. [c]Second-order rate constant for the reaction of [1-$^{13}$C]-GA catalyzed by the phosphite-liganded enzyme obtained from the fits of experimental data to eq 5 derived for Scheme 4. [d]Dissociation constant for release of phosphite dianion from the free enzyme obtained from the fits of experimental data to eq 5 derived for Scheme 4. [e]Dissociation constant for release of phosphite dianion from the transition state complex, calculated as described in the text. [f]Intrinsic dianion binding energy: $\Delta G^{‡} = -RT \ln K_d^{‡}$. [g]Third-order rate constant for the phosphite-activated TIM-catalyzed reaction of [1-$^{13}$C]-GA obtained from the fits of linear plots of $(k_{cat}/K_m)_{TIM}$ against $[HPO_3^{2-}]$. [h]Loop replacement mutation of TIM from chicken muscle [ref 29].

calculated using the total concentration of GAP in the enzyme assay. However, GAP exists largely (96%) in the hydrated form, and TIM is specific for the carbonyl form of this substrate (4%).[63] Values for $k_{cat}/K_m$ are also reported for catalysis of the reactive carbonyl form of GAP.

**TIM-Catalyzed Reaction of [1-$^{13}$C]-GA in $D_2O$.** The mutant *y*TIM-catalyzed reactions of [1-$^{13}$C]-GA in $D_2O$ were monitored by $^1$H NMR spectroscopy. These experiments provide the observed kinetic parameter $(k_{cat}/K_m)_{obs}$ (eq 1) for the TIM-catalyzed reaction of the carbonyl form of [1-$^{13}$C]-GA and the yield of the reaction products (Scheme 3). The product yields, determined at four different times during the first 20−30% of the reaction of [1-$^{13}$C]-GA, are invariant (±5%) over this time. The product yields for the reactions in the presence and absence of phosphite dianion catalyzed by wildtype *y*TIM, Y208T *y*TIM, Y208S *y*TIM, Y208A *y*TIM, Y208F *y*TIM, and S211A *y*TIM are reported in Tables S1−S6, respectively, of the Supporting Information to ref 28. The product yields for the reactions in the presence and absence of phosphite dianion catalyzed by S211G *y*TIM and Y208T/S211G *y*TIM are reported in Tables S1 and S2, respectively, of the Supporting Information to the present paper.

The value of $(k_{cat}/K_m)_{obs}$ for the TIM-catalyzed reactions of [1-$^{13}$C]-GA is equal to the sum of the second-order rate constants for the reactions that occur at the enzyme active site (Scheme 3A) and for nonspecific protein-catalyzed reactions (Scheme 3B).[47,64] The following procedures were followed to determine the true values of $(k_{cat}/K_m)_{TIM}$ for the unactivated and phosphite dianion-catalyzed reactions at the enzyme active site.

*Unactivated ([$HPO_3^{2-}$] = 0 M) yTIM-Catalyzed Reactions.* The slow unactivated reaction of [1-$^{13}$C]-GA in the presence of wildtype and mutants of *y*TIM gives the three products from reaction at the enzyme active site (Scheme 3A) along with significant yields of [1-$^{13}$C, 2,2-di-$^2$H]-GA and [1-$^{13}$C, 2-$^2$H]-GA. The latter products form by *nonspecific* protein-catalyzed reactions of [1-$^{13}$C]-GA outside the enzyme active site. This probably involves deuterium exchange into iminium ions formed by reaction of [1-$^{13}$C]-GA with surface lysine side chains (Scheme 3B).[47,62,64] It is not possible to distinguish [1-$^{13}$C, 2-$^2$H]-GA formed in the specific and nonspecific reactions and we therefore estimate the yield of [1-$^{13}$C, 2-$^2$H]-GA from Scheme 3A by assuming that the ratio of yields of [2-$^{13}$C, 2-$^2$H]-GA and [1-$^{13}$C, 2-$^2$H]-GA from the unactivated reaction is the same as for the phosphite dianion activated reaction, where little or no [1-$^{13}$C, 2,2-di-$^2$H]-GA (Scheme 3B) is generally observed.

$$\left(\frac{k_{cat}}{K_m}\right)_{TIM} = \left(\frac{k_{cat}}{K_m}\right)_{obs} f_E \quad (4)$$

The *true* second-order rate constants $(k_{cat}/K_m)_{TIM}$ for unactivated wildtype and mutant TIM-catalyzed reactions of the carbonyl form of [1-$^{13}$C]-GA to give [2-$^{13}$C]-GA, [2-$^{13}$C, 2-$^2$H]-GA, and [1-$^{13}$C, 2-$^2$H]-GA (Scheme 3A) were calculated using eq 4, where $f_E$ is the fractional yield of the products from reactions at the active site of TIM that are reported in Tables S1−S6 of ref 28 and in Tables S1 and S2 (Supporting Information) of this paper. The values of $(k_{cat}/K_m)_{TIM} = (k_{cat}/K_m)_E$ for the unactivated wildtype and mutant TIM-catalyzed reactions, determined at $[HPO_3^{2-}] = 0$ M are summarized in Table 2.

*Activation by Phosphite Dianion.* The second-order rate constants $(k_{cat}/K_m)_{TIM}$ (eq 4) for phosphite dianion activated wildtype and mutant *y*TIM-catalyzed reactions of the carbonyl form of [1-$^{13}$C]-GA are reported in Tables S1−S6 of ref 28 and in Tables S1 and S2 (Supporting Information) of this paper. Values of $f_E$ = 1.0 were determined for phosphite dianion activation of wildtype, Y208T, S211G, and Y208T/S211G *y*TIM catalyzed reactions of [1-$^{13}$C]-GA by ≥2.5 mM $HPO_3^{2-}$. The value of $f_E$ for the less active mutant enzymes increases with increasing concentration of the phosphite dianion activator, as the velocity of the activated reaction increases relative to the nearly constant unactivated reaction velocity. The following ranges of product yields were determined for the different TIMs over a 2.5−20 mM range of phosphite dianion concentrations: $f_E$ = 0.77−0.93, S211A *y*TIM; $f_E$ = 0.61−0.83, Y208S *y*TIM; $f_E$ = 0.70−0.90, Y208A *y*TIM; and $f_E$ = 0.07−0.22, Y208F *y*TIM.

Figure 2 shows the dependence of the values of $(k_{cat}/K_m)_{TIM}$ determined for wildtype and four mutant [S211G, Y208T/S211G, Y208T, S211A] *y*TIM-catalyzed reactions of [1-$^{13}$C]-GA on the concentration of added phosphite dianion. Figure 2 from ref 28 shows similar plots for reactions catalyzed by the


DOI: 10.1021/jacs.5b09328
J. Am. Chem. Soc. 2015, 137, 15185−15197

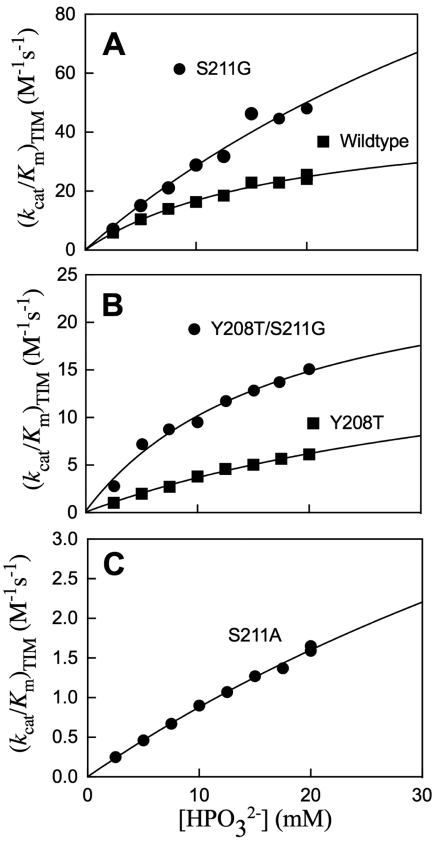


**Figure 2.** Dependence of second-order rate constants $(k_{cat}/K_m)_{TIM}$ for the TIM-catalyzed turnover of the free carbonyl form of [1-$^{13}$C]-GA in $D_2O$ on $[HPO_3^{2-}]$ at pD 7.0 and 25 °C at $I$ = 0.1, NaCl. The data were fitted to eq 5 derived for the model shown in Scheme 4. (A) Data for wildtype and S211G yTIM. (B) Data for Y208T and Y208T/S211G *y*TIM. (C) Data for S211A yTIM.

Y208A, Y208S, and Y208F mutant enzymes. The plots for the reactions catalyzed by Y208A, Y208F and S211A mutant *y*TIMs are linear. The values of $[(k_{cat}/K_m)_{E\bullet HPi}]/K_d$ determined as the slopes of these correlations are reported in Table 2. The solid lines through the experimental data for the Y208T, S211G, Y208T/S211G, and Y208S mutant enzymes show the nonlinear least-squares fits to eq 5, derived for Scheme 4 (S = [1-$^{13}$C]-GA), and using the values of $(k_{cat}/K_m)_E$ from Table 2 for the unactivated reaction in the absence of phosphite dianion. These fits give $(k_{cat}/K_m)_{E\bullet HPi}$ for turnover of [1-$^{13}$C]-GA by E·$HPO_3^{2-}$ and $K_d$ for release of phosphite dianion from E·$HPO_3^{2-}$ (Table 2). We note the large uncertainty in these kinetic parameters when $K_d \geq 40$ mM (Y208T, S211G, and Y208S mutants), which is substantially greater that the largest $[HPO_3^{2-}]$ = 20 mM used in these experiments.

**Scheme 4**

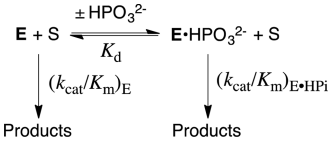


$$\left(\frac{k_{cat}}{K_m}\right)_{TIM} = \left(\frac{K_d}{K_d + [HPO_3^{2-}]}\right)\left(\frac{k_{cat}}{K_m}\right)_E + \left(\frac{[HPO_3^{2-}]}{K_d + [HPO_3^{2-}]}\right)\left(\frac{k_{cat}}{K_m}\right)_{E\bullet HPi} \quad (5)$$

## DISCUSSION

The kinetic parameters for isomerization of GAP catalyzed by Y208F and S211A mutants of *y*TIM (Table 1) are in good agreement with previously published values.[44] The effects of these mutations on the activation barrier $\Delta G^{\ddagger}$ for the isomerization of GAP catalyzed by wildtype enzyme are shown on Figure 3. The simplest interpretation of the effect of a Y208F mutation, which eliminates the intraloop hydrogen bond between the hydroxyl group of Y208 and the amide nitrogen of A176, is that this hydrogen bond provides a 4.4 kcal/mol stabilization of the isomerization reaction transition state.[44,65,66] However, this hydrogen bond is eliminated by the Y208A mutation, whose smaller effect on $\Delta G^{\ddagger}$ compared with Y208F shows that the phenyl group of Y208 is held in an active conformation by the hydrogen bond to the phenol hydroxyl, and relaxes to a second conformation at the Y208F mutant, where the enzyme activity is reduced by ca. 50-fold compared to the Y208A and Y208S mutants. These results are consistent with the notion that the binding energy from the hydrogen bond to the phenol hydroxyl is utilized to hold the phenyl group in a conformation that reduces the dielectric constant for the active site cage,[27] and optimizes stabilizing electrostatic interactions between the transition state and the protein catalyst. The S211A and S211G mutations of TIM each eliminate intraloop hydrogen bonds to the side-chain hydroxyl, yet show different effects on enzyme activity (Figure 3). The explanation for the effects of Y208 and S211 mutations will be considered in greater detail in later sections of this paper.

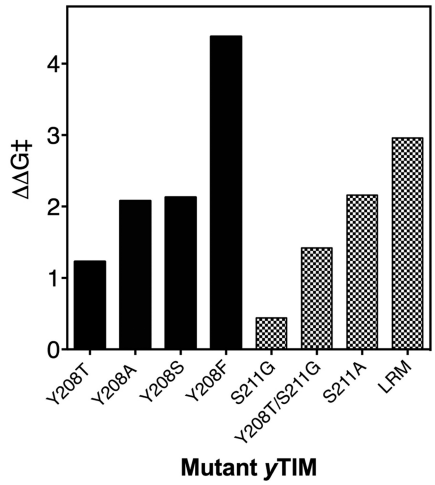


**Figure 3.** Bar graph which compares the effect of mutations of Y208 and S211 on the activation barrier to TIM-catalyzed isomerization of GAP, calculated from values $k_{cat}/K_m$ for the wildtype and mutant enzymes (Table 1).

There are two additional recent examples of the difficulty in obtaining reliable estimates, from the effect of a single point mutation, of the contribution of side-chain hydrogen bonds to


DOI: 10.1021/jacs.5b09328
J. Am. Chem. Soc. 2015, 137, 15185−15197

stabilization of the transition states for enzyme-catalyzed proton transfer and decarboxylation reactions.

(1) The Y16F mutation at ketosteroid isomerase from *P. putida*[53,54] eliminates the side-chain hydrogen bond to the dienolate oxyanion intermediate. The ca. 100-fold larger decrease in $k_{cat}/K_m$ for Y16F, compared with Y16A, Y16G, Y16S, and Y16T mutations was proposed to reflect the relief of destabilizing hydrophobic interactions between the phenyl side chain and the intermediate oxyanion at the latter four mutants, along with formation of a hydrogen bond to a water molecule at the cavity created by removal of the side-chain phenyl ring.

(2) The caged complex between yeast orotidine 5′-monophosphate decarboxylase (*Sc*OMPDC) and OMP is stabilized by an interaction between the side chain of Y217 and the substrate phosphodianion, but now the 60-fold reduction in $k_{cat}/K_m$ determined for the Y217F mutant[31,32] is *smaller* than the 4400-fold effect of a Y217A mutation.[67,68] These and many other experimental results are consistent with minimal destabilizing hydrophobic interactions between the phosphodianion and the phenyl side chain of the Y217F mutant, so that the contribution of the phenol hydrogen bond to catalysis may be estimated from the effect of the Y217F mutation on OMPDC-catalyzed decarboxylation of OMP.[67,68] The side-chain of Y217 lies in a flexible loop that folds over the substrate phosphodianion. The Y217A mutation results in a large decrease in the rate of loop closure of the phosphodianion, so that this conformational change becomes rate-determining for decarboxylation of OMP.[69]

**Reactions of the Substrate in Pieces.** Rate constants for reactions that proceed through structurally related transition states often show linear logarithmic correlations that are referred to as linear free energy relationships (LFER).[70,71] The slopes of these linear relationships provide a detailed characterization of the structures of transition states for enzymatic reactions that is difficult or impossible to obtain by other methods.[72−75] The TIM-catalyzed isomerization of GAP, with second-order rate constant $(k_{cat}/K_m)_{GAP}$, differs from the TIM-catalyzed reaction of the substrate pieces GA + $HP_i$, with third-order rate constant $k_{cat}/K_{HPi}K_{GA}$ (Scheme 5), by the

**Scheme 5**

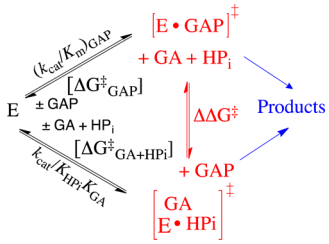


presence of the covalent connection between the pieces. Figure 4 presents the excellent linear logarithmic free energy correlation between these rate constants, with the slope 1.04 ± 0.03. A large positive deviation from this correlation is observed for the L232A mutant. The L232 mutation results in a large increase in $k_{cat}/K_{HPi}K_{GA}$, but there can be no similar increase in $(k_{cat}/K_m)_{GAP}$, because the wildtype TIM-catalyzed reaction of GAP is partly diffusion limited.[50,51] A smaller positive deviation is observed for the 208-TGAG for 208-YGGS loop replacement mutation (LRM). This point is arbitrarily excluded in order to emphasize the excellent quality of the correlation of data for the single and double mutant enzymes.

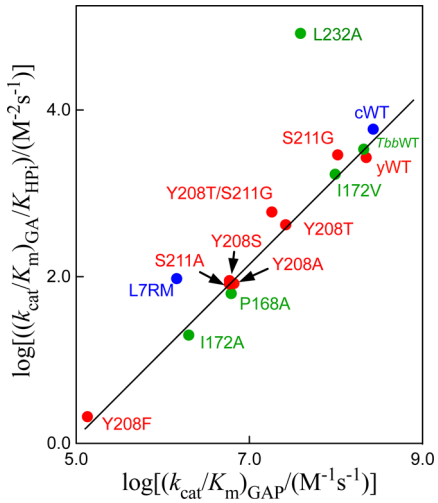


**Figure 4.** Linear free energy relationship, with slope 1.04 ± 0.03, between the second-order rate constant log $(k_{cat}/K_m)_{GAP}$ for wildtype and mutant TIM-catalyzed isomerization of GAP and the corresponding third-order rate constant log $(k_{cat}/K_{HPi}K_{GA})$ for the enzyme-catalyzed reactions of the substrate pieces GA and $HP_i$. Key: green symbols, mutants of TIM from *Trypanosoma brucei* (*Tbb*TIM); blue symbols, mutants of TIM from chicken muscle (*c*TIM); red symbols, mutants of *y*TIM.

The linear correlation from Figure 4 shows that most mutations result in the *same* destabilization of the transition states for the catalyzed reactions of the whole substrate $[\Delta\Delta G^{\ddagger}_{GAP}]$ and substrate pieces $[\Delta\Delta G^{\ddagger}_{GA+HPi}]$. We conclude that these two transition states show strikingly similar interactions with loop 6 and 7 of TIM, and are remarkably similar by this criterion. The slope of 1.0 for Figure 4 requires a constant difference in activation barriers for the two reactions of $\Delta\Delta G^{\ddagger}$ = 6.6 ± 0.3 kcal/mol (Scheme 5). This energetic advantage was recently noted in other systems,[76] and represents partly or entirely the entropic advantage to the binding of the transition state for the reaction of the whole substrate, compared with the reaction of the substrate in pieces.[77]

Inspection of X-ray crystal structures of the complexes between TIM and DHAP (Figure 5A)[22,78] or the intermediate analogues phosphoglycolate[23,79] and phosphoglycolohydroxamate,[24,26] suggests that elimination of the linkage that connects the substrate pieces (Figure 5B) might not have a large effect on interactions between the enzyme and reaction transition states. However, these phosphodianion interactions were implicitly assumed to form fully at the Michaelis complex, so that examination of these X-ray crystal structures failed to provide the insight necessary to predict enzyme activation by phosphite dianion and the third-order TIM-catalyzed reaction of the substrate pieces. We suggest that further critical evaluations of implicit assumptions made when examining X-ray crystal structures might provide the necessary insight for the design of important experimental studies on enzyme mechanisms.

We conclude that there is similar strong activation of TIM by interactions with the phosphodianion of whole substrate and the phosphite dianion piece. The question is *how are these interactions utilized for the purpose of enzyme activation?* The open conformation of TIM ($E_O$, Scheme 6) is essentially inactive, so that activation reflects the high specificity of both the dianion and the transition state for binding the high-energy active closed form of TIM ($E_C$, Scheme 6).[41] The ≈1000 fold


DOI: 10.1021/jacs.5b09328
J. Am. Chem. Soc. 2015, 137, 15185−15197

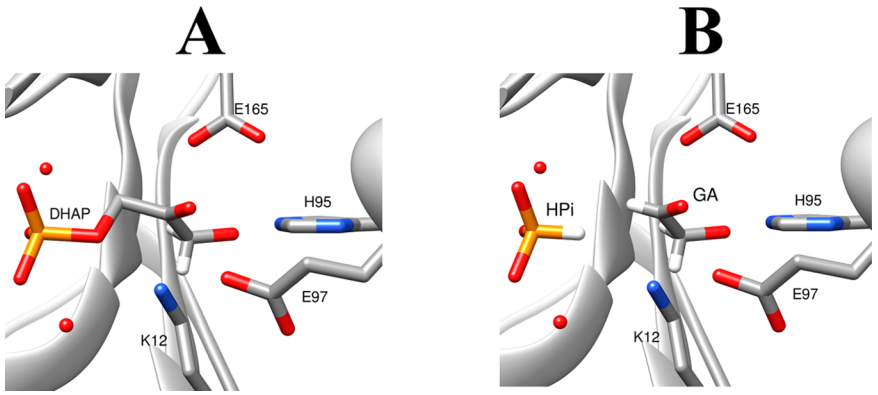


**Figure 5.** (A) Representation showing the active site of *y*TIM, in a complex with DHAP, from the X-ray crystal structure of McDermott and co-workers (PDB entry 1NEY). This structure provides an *optimal orientation* of the carboxylate side chain of the catalytic base (E165), the imidazole side chain of the active site electrophile (H95), and the alkyl ammonium side chain of K12. (B) Hypothetical representation showing *y*TIM in complex with phosphite dianion and glycolaldehyde, generated in silico from (A) by eliminating the covalent connection at DHAP.

**Scheme 6**

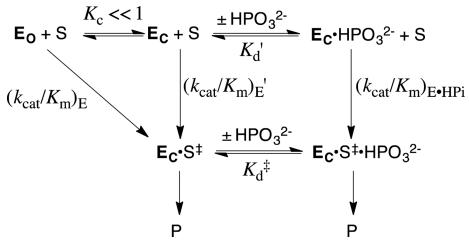


activation of TIM by phosphite dianion reflects the utilization of 4-kcal/mol out of a total 12 kcal/mol dianion binding energy to drive the unfavorable protein conformational change from $E_O$ to $E_C$. The barrier to formation of the catalytically active caged complexes [$E_C \cdot S^{\ddagger}$, $E_C \cdot HPO_3^{2-}$, and $E_C \cdot S^{\ddagger} \cdot HPO_3^{2-}$) is due, minimally, to the enthalpic cost of desolvation of the active site and the entropic cost of freezing the motion of flexible protein loops and the catalytic side chains.[27,42] The binding energy of the whole substrate GAP is also utilized to drive the same activating conformational change. The difference between the modest observed binding energy $\Delta G_{obs}$ for GAP, calculated from the Michaelis constant $K_m$, and the larger intrinsic substrate binding energy $\Delta G_{int}$, is equal to the binding energy that is utilized to drive the enzyme conformational change $[-RT \ln(1/K_C)]$.[80,81]

**The Roles for Y208 and S211 in Catalysis by TIM.** The ligand-driven closure of loops 6 [residues 166−176] and 7 [208-YGGS-211] moves the S211 hydroxyl into position to hydrogen bond with the backbone carbonyl oxygen and amide nitrogen from A169 and G173, respectively; the backbone NH group of S211 into a position to hydrogen bond with the ligand phosphodianion; and the Y208 hydroxyl into a position to hydrogen bond to the backbone amide nitrogen from A176 (Figure 6).[5,42−44] Knowles and Sampson proposed that the side chains of Y208 and S211 stabilize the loop closed form of TIM $E_C$ (Scheme 6) relative to the open form $E_O$, and concluded on the basis of the large effects of Y208F and S211A mutations on catalysis (see Figure 3) that these intraloop interactions play a role in catalysis.[44,65]

Cutting the substrate into dianion and carbon acid pieces allows separate determination of the effects of mutations on transition state stabilization from interactions at the dianion activation site and the catalytic site.[29] Different effects are

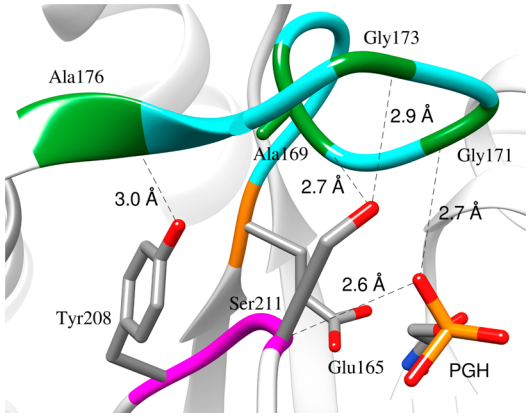


**Figure 6.** Representation of the structure of the closed form of TIM liganded with PGH (PDB entry 1TPH),[24] an analogue of the enediolate reaction intermediate. The hydrogen bonds between the hydroxyl of Y208 (loop 7) and the amide of A176 (loop 6), and between the hydroxyl of S211 and the carbonyl oxygen and amide nitrogen from A169 and G173, respectively are shown.[5,43]

possible, depending upon the affected site. (i) Mutations that alter the structure of the dianion activation site will cause a decrease in $K_d^{\ddagger}$ for release of the dianion at the ternary transition state complex (eq 6, derived for Scheme 7).[29] (ii)

**Scheme 7**

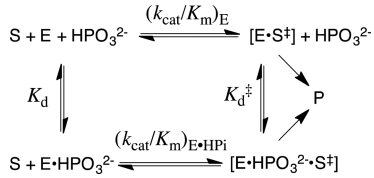


Mutations that alter the substrate reactivity at the catalytic site will cause a decrease in $(k_{cat}/K_m)_E$ for deprotonation of glycolaldehyde.[29] (iii) Mutations that cause a change in $K_C$ (Scheme 6) by changing the stability of $E_C$ relative to $E_O$ will result in equal changes in $(k_{cat}/K_m)_E = (k_{cat}/K_m)_E'(K_C)$ and $(K_d) = (K_d')/(K_C)$ (Scheme 6). This has been observed in studies on the L232A mutant of *TbbTIM*.[50,51]



DOI: 10.1021/jacs.5b09328
J. Am. Chem. Soc. 2015, 137, 15185−15197

$$K_d^{\ddagger} = \frac{K_d(k_{cat}/K_m)_E}{(k_{cat}/K_m)_{E\bullet HPi}} \quad (6)$$

An examination of the kinetic parameters for wildtype, Y208 or S211 mutant enzyme-catalyzed reactions of the substrate pieces shows the following effects, which are summarized in Table 3.

**Table 3. Localization of the Effects of Mutations of *y*TIM on the Catalyzed Reactions of the Substrate Pieces, Determined As Described in the Text**

| | | $[(k_{cat}/K_m)_E]_{obs}$[b] | |
|---|---|---|---|
| mutant TIM | intrinsic dianion binding energy ($-RT\ln(K_d^{\ddagger})$)[a] | $(k_{cat}/K_m)_E'$[c] | $K_C$[d] |
| Y208T | ↓ | no change | no change |
| Y208S | ↓ | no change | no change |
| Y208A | ↓ | no change | no change |
| Y208F | ↓ | ↓ | no change |
| S211A | no change | no change | ↓ |
| S211G | small decrease[e] | no change | no change |
| Y208T/S211G | ↓ | small increase | no change |
| 208-TGAG for 208-YGGS (LRM)[f] | small decrease[e] | ↓ | no change |
| P168A[g] | no change | ↓ | no change |

[a]The intrinsic dianion binding energy, calculated from data reported in Table 2 using eq 6 derived for Scheme 7. [b]The observed rate constant for enzyme-catalyzed reactions of the truncated substrate glycolaldehyde; $[(k_{cat}/K_m)_E]_{obs} = (k_{cat}/K_m)_E'(K_C)$ where $(k_{cat}/K_m)_E'$ is the second-order rate constant for the reactions of glycolaldehyde catalyzed by the closed form of TIM (Scheme 6). It is assumed when there is no change in $[(k_{cat}/K_m)_E]_{obs}$ for a mutant enzyme, that there is no effect of the mutation on either $(k_{cat}/K_m)_E'$ or $(K_C)$. [c]The true second-order rate constant for the reactions of glycolaldehyde catalyzed by the closed form of TIM (Scheme 6). [d]The equilibrium constant for conversion of the inactive open form of TIM ($E_O$) to the active closed enzyme ($E_C$, Scheme 6). [e]An approximate 0.4 kcal/mol decrease. [f]Loop replacement mutation of TIM from chicken muscle.[29,82] [g]The P168A mutation of TIM from *T. brucei*.[29,83]

(1) The mutations of Y208 cause a decrease in $K_d^{\ddagger}$ for release of the dianion from the ternary transition state complex, which correspond to 0.4−2.4 kcal/mol decreases in the intrinsic phosphite dianion binding energy $\Delta G^{\ddagger}$ (Table 2). This provides direct evidence that Y208 is required for robust enzyme activation by dianions. With the exception of Y208F, these mutations do not cause large changes $(k_{cat}/K_m)_E$ for unactivated deprotonation of GA.

(2) The S211A mutation results in a 60-fold *decrease* in $(k_{cat}/K_m)_E$ for deprotonation of glycolaldehyde, increases in the values of $K_d$ and $K_m$ for release of phosphite dianion and GAP from the free enzyme, but little change in $K_d^{\ddagger}$ for release of phosphite dianion from the transition state complex (Table 2 and Scheme 6). These changes are consistent with a decrease in $K_C$ for the Y211A mutant enzyme conformational change (Scheme 6). This results in utilization of a greater fraction of the total dianion binding energy, which remains nearly constant (Table 2), to drive the conformational change. By contrast, the S211G mutation eliminates the same hydrogen bond contact as S211A, and results in only small changes in the kinetic parameters for the TIM-catalyzed reactions of whole substrate and the substrate in pieces. The S211 side chain lies at the surface of TIM, where it is exposed to solvent. We suggest that loop-6 hydrogen-bonding interactions with water substitute for interactions with the excised $-CH_2OH$ side chain to provide a significant stabilization of the loop-closed enzyme.

(3) The Y208F mutation results in a decrease in the total dianion binding energy and in $(k_{cat}/K_m)_E = (k_{cat}/K_m)_E'K_C$ for carbon deprotonation at the catalytic site (Scheme 7). There is only a small increase in $K_m$ for isomerization of GAP, so that the mutation does not cause a large change in $K_C$ for the enzyme conformational change. We conclude that this mutation results in a decrease in $(k_{cat}/K_m)_E'$ for deprotonation of GA (see following section).

It is interesting that mutations of both Y208 and S211 eliminate intraloop hydrogen bonds, which appear to stabilize the closed form of TIM, but only the S211A mutation shows effects on kinetic parameters for reactions of the substrate pieces that are consistent with a decrease in $K_C$ for loop closure. The minimal two-state model shown in Scheme 6 provides a satisfactory rationalization of the effects of a wide range of mutations on the kinetic parameters for reactions catalyzed by TIM, OMPDC and GPDH.[12,28,29,31,35,50,51,69,84,85] However, in this case, the model is consistent with the implausible conclusion that Y208 mutations, which eliminate a hydrogen bond that stabilizes $E_C$ (Figure 6), have no effect on $K_C$ but result in a reduction in the intrinsic dianion binding energy $\Delta G^{\ddagger} = -RT\ln(K_d^{\ddagger})$. We propose, as a more plausible explanation for these results, that this dianion binding energy is used to stabilize an alternative closed conformation $E_C'$ for the Y208 mutant enzymes, which is more stable than $E_C$, but for which there is a smaller total dianion binding energy -$\Delta G^{\ddagger}$. In any case, the minimal model from Scheme 6 will break down in cases where there are two conformations of the closed enzyme ($E_C$ and $E_C'$), which each show catalytic activity, and where site directed mutations stabilize $E_C'$ relative to the $E_C$, the active form for wildtype TIM. We also note that in contrast with the solvent exposed side chain of S211, the side chain of Y208 is buried beneath loop 6 at $E_C$. We suggest that the movement of 208 mutant side chains is constrained and/or coupled to shifts in the position of its neighbors in a manner that we are unable to deal with in this paper.

**A Second Linear Free Energy Relationship.** The activation of TIM by interactions with bound dianions is reflected in the values of $K_d^{\ddagger}$ and $k_{cat}$, respectively, for reactions of the pieces (Scheme 7) and whole substrate. Figure 7 shows the logarithmic linear free energy relationship between $K_d^{\ddagger}$ for activation by phosphite dianion (Table 2) and $k_{cat}$ for catalysis of the reaction of GAP (Table 1) catalyzed by wildtype and many loop 7 mutant enzymes. The slope of the correlation, 0.53 ± 0.16, shows that ca. 50% of the phosphite dianion binding energy lost due to mutations at loop 7 is expressed as a reduction in the enzyme-activating phosphodianion binding energy for mutant TIM-catalyzed isomerization of the *whole* substrate GAP. The remaining ca. 50% is expressed at the ground state Michaelis complex of wildtype *y*TIM to GAP.[41]

Large negative deviations from the linear correlation shown in Figure 7 are observed for three mutants: Y208F, P168A,[29] and the 208-TGAG for 208-YGGS LRM.[29] These negative deviations reflect the substantial effects of these mutation on substrate reactivity at the catalytic site, which result in decreases in *both* $(k_{cat}/K_m)_E$ for catalysis of the unactivated reaction and


DOI: 10.1021/jacs.5b09328
J. Am. Chem. Soc. 2015, 137, 15185−15197

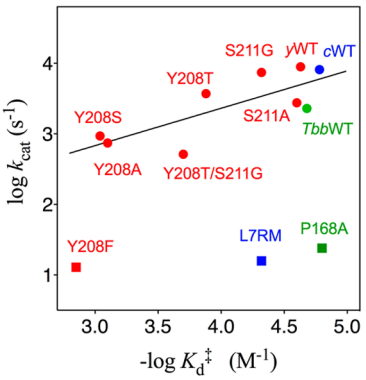


**Figure 7.** Logarithmic correlation between values of $k_{cat}$ for *y*TIM catalyzed isomerization of GAP and the intrinsic dianion binding energy for phosphite dianion activation of wildtype and mutant TIM-catalyzed reactions of [1-$^{13}$C]-GA. Key: green symbols, mutants of TIM from *T. brucei* (*Tbb*TIM); blue symbols, mutants of TIM from chicken muscle (*c*TIM); red symbols, mutants of *y*TIM.

in $k_{cat}$ for catalysis of the reaction of the whole substrate, but which do not affect the dianion binding energy $-RT\ln(K_d^{\ddagger})$. For example, the 20-fold smaller value of $(k_{cat}/K_m)_E$ for Y208F mutant compared to the wildtype *y*TIM-catalyzed reaction of glycolaldehyde, is similar to the 40-fold reduction in $k_{cat}$ implied by the 1.6 log unit negative deviation of this mutant enzyme from the correlation in Figure 7. By contrast, the S211A mutation results in a 30-fold reduction of the observed kinetic parameter $(k_{cat}/K_m)_E$ compared with wildtype TIM, but much smaller changes in $k_{cat}$ and $K_d^{\ddagger}$, so that the data for this mutant appear to lie on the correlation shown in Figure 7. This is consistent with the above conclusion that the change in the *observed* kinetic parameter $(k_{cat}/K_m)_E$ is due to a decrease in $K_C$ (Scheme 6) for the enzyme conformational change, rather than a decrease in the *microscopic* rate constant $(k_{cat}/K_m)_E'$ for the reaction of glycolaldehyde catalyzed by the active closed form of TIM (Table 3). The exclusion of S211A from the linear correlation shown in Scheme 7 results in an increase in the slope of the correlation from 0.53 ± 0.16 to 0.57 ± 0.17.

The large effect of the Y208F mutations on the kinetic parameters for *y*TIM catalyzed reactions of whole substrates and substrate pieces represents the sum of the effects of this mutation on dianion activation ($K_d^{\ddagger}$) and on catalysis ($[k_{cat}/K_m)_E]$, Table 3). By comparison, the effect of the P168A mutation of *Tbb*TIM is localized to the catalytic site. It is the result of the loss of a steric clash between the side chain of P168 and the carbonyl oxygen of G211, which drives the 2 Å shift in the position of the carboxylate side chain of E167 from the low activity swung-out position for open unliganded TIM to the active swung-in position at the closed wildtype enzyme.[83] The catalytic base is observed to lie at the swung-out position for the P168A mutant enzyme. This change in the position of this base affects mainly the kinetic parameters $(k_{cat}/K_m)_E$ and $k_{cat}$ for deprotonation of glycolaldehye and GAP respectively, but results in little change in $K_d^{\ddagger}$ for phosphite dianion binding and in $K_m$ for the isomerization of GAP.[29]

The large negative deviation from Figure 7 observed for the 208-TGAG for 208-YGGS loop 7 replacement mutation (LRM) at TIM also reflects the large effect of the mutation on the values of $(k_{cat}/K_m)_E$ and $k_{cat}$ for reaction at the catalytic site compared to the small effect on $K_d^{\ddagger}$ (Table 2).[29] Our data show that complex changes in the kinetic parameters for the wildtype TIM-catalyzed reaction of the substrate pieces are observed when the 208-TGAG for 208-YGGS loop 7 replacement is carried out as consecutive point mutations (Tables 2 and 3). The initial Y208T mutation affects mainly $K_d^{\ddagger}$ for dianion binding, the second Y208T/S211G mutation is conservative, and the final G210A substitution at this double mutant results in a large decrease in $(k_{cat}/K_m)_E$, while restoring most of the transition state dianion binding energy $[-RT\ln(K_d^{\ddagger})]$ lost on the first two point mutations. These data cannot be rationalized without additional structural data. They represent an interesting benchmark against which to test the ability of computational methods to model experimental data on TIM, and the opportunity to use computational methods to provide genuine insight into the relationship between TIM structure and function.

**Broader Issues.** *Active Site Architecture.* An important goal of this research is to characterize the similarities and differences in the active-site architecture of three enzymes, which catalyze chemically distinct reactions, but show similar strong activation for catalysis by dianions; TIM,[16] orotidine 5′-monophosphate decarboxylase (OMPDC),[33,86] and glycerol 3-phosphate dehydrogenase (GPDH).[30,34] We find that the effects of most TIM mutations may be localized to either effects on the intrinsic dianion binding energy or effects on catalysis (Table 3). This is consistent with the division of the substrate binding pocket into distinct dianion activation and catalytic sites.[29] However, the close proximity of these sites allows: (1) The cationic side chain of Lys-12 to interact with both the bound phosphodianion, through an intervening water molecule, and the carbonyl oxygen of DHAP.[48,49,87] (2) The effect of some mutations, such asY208F (Table 3), spans these two sites. By comparison, the greater separation between the substrate phosphodianion and orotate ring of orotidine 5′-monophosphate has allowed for evolution of well-separated dianion activation and catalytic sites at orotidine 5′-monophosphate decarboxylase.[88] Now the effects of mutations of amino acid side-chains, which interact with the substrate phosphodianion, are expressed exclusively as changes in the intrinsic dianion binding energy.[31,32]

*Evolution of the TIM Barrel.* The classic TIM-barrel $(\beta\alpha)_8$ fold has a plastic, or floppy, structure conferred by 16 flexible loops, which connect 16 rigid $\alpha$ (eight) and $\beta$ (eight) secondary structural elements.[40] These flexible loops enable TIM barrel proteins to access the inestimable number of conformations needed to obtain catalysis of a broad range of reactions. We propose that the conformational change required to *mold* floppy loops 6 and 7 of the eponymous TIM barrel to the rigid caged catalytic complex is uphill thermodynamically, in part because of the intrinsically disordered state of the unliganded protein.[27,40,42] This role for nonreacting substrate fragments is generalizable to any TIM barrel-catalyzed reaction where a ligand-induced conformational change is observed.[27,41] In the case of TIM, once the essential function of driving the conformational change has been performed, the dianion becomes a spectator, and the catalyzed reaction proceeds with equal efficiency for the whole substrate and substrate pieces (Figures 4 and 5A, B).

*A Role for Protein Dynamics?* Transition state theory provides a useful framework for the interpretation of the complex effects of loop 7 mutations on the TIM-catalyzed reactions of whole and truncated substrates. However, a role for *dynamics* must also be considered, since almost anything done to a protein changes protein dynamics, so that an explanation for any experimental result is immediately at hand.[89−93] Loop 7


DOI: 10.1021/jacs.5b09328
J. Am. Chem. Soc. 2015, 137, 15185−15197

[208-YGGS-211] participates in the phosphodianion driven conformational change from an open enzyme $E_O$ to the closed form $E_C$ where the side chains from Y208 and S211 form hydrogen bonds to the backbone of loop 6 (Figure 6). The dynamics of the motion of loop 6 has been probed in computational[94,95] and experimental studies.[96−99] We consider whether our experimental results provide any evidence to support the hypothesis that motions of loop 6 and 7 promote proton transfer reaction at the catalytic site, which is 8−9 Å removed from the altered loop 7 side chains.[89−91]

The major *apparent* effect of mutations of Y208 is to cause a reduction in the intrinsic dianion binding energy (Table 2). This is consistent with a role for the hydrophobic side chain of Y208 in maintaining a low effective dielectric constant at the dianion activation site, which enables optimal interactions between the protein catalyst and the polar isomerization reaction transition state. Mutations of Y208 might interfere with a vibrational motion that promotes catalysis, but this effect could only be important when phosphite dianion is bound to the enzyme, because most the mutations cause no change in $(k_{cat}/K_m)_E$ for the reaction in the absence of this dianion (Table 2). The excellent linear free energy correlation between the rate constants for reactions of the whole substrate and pieces (Figure 4) shows there is no transmission of the energy of a hypothetical promoting vibrational motion through the covalent bond that connects these pieces in the whole substrate.

The major effect of the S211A mutation is to reduce the phosphodianion binding energy expressed at Michaelis complexes, while maintaining a nearly constant intrinsic dianion binding energy (Tables 1 and 2). These results are consistent with stabilization of $E_O$ relative to $E_C$ at the S211A mutant, so that a larger fraction of the total dianion binding energy is required to drive the protein conformational change. It difficult or impossible to rationalize the effects of mutations at both Y208 and S211 as originating from changes in promoting vibrational modes, since in one case (Y208) the mode only promotes the reaction at the complex which contains the dianion [$(k_{cat}/K_m)_E$ is invariant, Table 2], while in the other (S211) the mode would act to cause similar increases in $(k_{cat}/K_m)_E$ and in $(k_{cat}/K_m)_{HPi}/K_d$ for reactions in the absence and presence of phosphite dianion, respectively (Table 2).

Sampson and Knowles observed a solvent viscosity dependence on $k_{cat}/K_m$ for Y208F mutant TIM-catalyzed isomerization of GAP, and a large primary deuterium kinetic isotope effect of $k_H/k_D$ = 6 on $k_{cat}/K_m$ for TIM-catalyzed isomerization of [1-$^2$H]-dihydroxyacetone phosphate.[65] The first result is consistent with a viscosity-dependent rate limiting conversion of open $E_O$ to closed $E_C$, while the second requires that substrate deprotonation be rate determining for the mutant enzyme-catalyzed proton transfer reaction. Sampson and Knowles proposed either that, "*loop closure and deprotonation are coupled and occur in the same rate-limiting step or that these two processes happen sequentially but interdependently.*" Y208F is the only mutation at position 208 that results in a large decrease in the reactivity of glycolaldehyde at the catalytic site (Table 3). This is consistent either with the notion that the barrier to conversion of $E_O$ to $E_C$ somehow contributes to the overall activation barrier for the Y208A mutant enzyme-catalyzed deprotonation of GA, or with an effect of the mutation on enzyme structure that extends to the catalytic site.

## ■ ASSOCIATED CONTENT

### Supporting Information

The Supporting Information is available free of charge on the ACS Publications website at DOI: 10.1021/jacs.5b09328.

Tables S1 and S2, second-order rate constant and fractional product yields for the reaction of [1-$^{13}$-C]-GA catalyzed by S211G (Table S1) and Y208T/S211G (Table S2) mutant TIM (PDF)

## ■ AUTHOR INFORMATION


### Corresponding Author

*jrichard@buffalo.edu


### Notes

The authors declare no competing financial interest.

## ■ ACKNOWLEDGMENTS

We acknowledge the National Institutes of Health Grant GM39754 for generous support.

## ■ REFERENCES


(1) Knowles, J. R. *Philos. Trans. R. Soc., B* **1991**, *332*, 115−121.
(2) Knowles, J. R. *Nature (London, U. K.)* **1991**, *350*, 121−124.
(3) Knowles, J. R.; Albery, W. J. *Acc. Chem. Res.* **1977**, *10*, 105−111.
(4) Richard, J. P. *Biochemistry* **2012**, *51*, 2652−2661.
(5) Wierenga, R. K. *Cell. Mol. Life Sci.* **2010**, *67*, 3961−3982.
(6) Jencks, W. P. *Catalysis in Chemistry and Enzymology*; Dover Publications: Mineola, NY, 1987.
(7) Richard, J. P. *J. Am. Chem. Soc.* **1984**, *106*, 4926−4936.
(8) Waley, S. G.; Miller, J. C.; Rose, I. A.; O'Connell, E. L. *Nature (London, U. K.)* **1970**, *227*, 181.
(9) De la Mare, S.; Coulson, A. F. W.; Knowles, J. R.; Priddle, J. D.; Offord, R. E. *Biochem. J.* **1972**, *129*, 321−331.
(10) Straus, D.; Raines, R.; Kawashima, E.; Knowles, J. R.; Gilbert, W. *Proc. Natl. Acad. Sci. U. S. A.* **1985**, *82*, 2272−2276.
(11) Zhang, Z.; Komives, E. A.; Sugio, S.; Blacklow, S. C.; Narayana, N.; Xuong, N. H.; Stock, A. M.; Petsko, G. A.; Ringe, D. *Biochemistry* **1999**, *38*, 4389−4397.
(12) Malabanan, M. M.; Nitsch-Velasquez, L.; Amyes, T. L.; Richard, J. P. *J. Am. Chem. Soc.* **2013**, *135*, 5978−5981.
(13) Lodi, P. J.; Chang, L. C.; Knowles, J. R.; Komives, E. A. *Biochemistry* **1994**, *33*, 2809−2814.
(14) Komives, E. A.; Chang, L. C.; Lolis, E.; Tilton, R. F.; Petsko, G. A.; Knowles, J. R. *Biochemistry* **1991**, *30*, 3011−3019.
(15) Nickbarg, E. B.; Davenport, R. C.; Petsko, G. A.; Knowles, J. R. *Biochemistry* **1988**, *27*, 5948−5960.
(16) Amyes, T. L.; Richard, J. P. *Biochemistry* **2007**, *46*, 5841−5854.
(17) Amyes, T. L.; O'Donoghue, A. C.; Richard, J. P. *J. Am. Chem. Soc.* **2001**, *123*, 11325−11326.
(18) Richard, J. P.; Amyes, T. L. *Curr. Opin. Chem. Biol.* **2001**, *5*, 626−633.
(19) Morrow, J. R.; Amyes, T. L.; Richard, J. P. *Acc. Chem. Res.* **2008**, *41*, 539−548.
(20) Pompliano, D. L.; Peyman, A.; Knowles, J. R. *Biochemistry* **1990**, *29*, 3186−3194.
(21) Bash, P. A.; Field, M. J.; Davenport, R. C.; Petsko, G. A.; Ringe, D.; Karplus, M. *Biochemistry* **1991**, *30*, 5826−5832.
(22) Jogl, G.; Rozovsky, S.; McDermott, A. E.; Tong, L. *Proc. Natl. Acad. Sci. U. S. A.* **2003**, *100*, 50−55.
(23) Lolis, E.; Petsko, G. A. *Biochemistry* **1990**, *29*, 6619−6625.
(24) Zhang, Z.; Sugio, S.; Komives, E. A.; Liu, K. D.; Knowles, J. R.; Petsko, G. A.; Ringe, D. *Biochemistry* **1994**, *33*, 2830−2837.
(25) Davenport, R. C.; Bash, P. A.; Seaton, B. A.; Karplus, M.; Petsko, G. A.; Ringe, D. *Biochemistry* **1991**, *30*, 5821−5826.
(26) Alahuhta, M.; Wierenga, R. K. *Proteins: Struct., Funct., Genet.* **2010**, *78*, 1878−1888.




DOI: 10.1021/jacs.5b09328
*J. Am. Chem. Soc.* 2015, 137, 15185−15197

(27) Richard, J. P.; Amyes, T. L.; Goryanova, B.; Zhai, X. *Curr. Opin. Chem. Biol.* **2014**, *21*, 1−10.
(28) Zhai, X.; Amyes, T. L.; Richard, J. P. *J. Am. Chem. Soc.* **2014**, *136*, 4145−4148.
(29) Zhai, X.; Amyes, T. L.; Wierenga, R. K.; Loria, J. P.; Richard, J. P. *Biochemistry* **2013**, *52*, 5928−5940.
(30) Reyes, A. C.; Zhai, X.; Morgan, K. T.; Reinhardt, C. J.; Amyes, T. L.; Richard, J. P. J. *J. Am. Chem. Soc.* **2015**, *137*, 1372−1382.
(31) Goldman, L. M.; Amyes, T. L.; Goryanova, B.; Gerlt, J. A.; Richard, J. P. *J. Am. Chem. Soc.* **2014**, *136*, 10156−10165.
(32) Amyes, T. L.; Ming, S. A.; Goldman, L. M.; Wood, B. M.; Desai, B. J.; Gerlt, J. A.; Richard, J. P. *Biochemistry* **2012**, *51*, 4630−4632.
(33) Spong, K.; Amyes, T. L.; Richard, J. P. *J. Am. Chem. Soc.* **2013**, *135*, 18343−18346.
(34) Tsang, W.-Y.; Amyes, T. L.; Richard, J. P. *Biochemistry* **2008**, *47*, 4575−4582.
(35) Reyes, A. C.; Koudelka, A. P.; Amyes, T. L.; Richard, J. P. *J. Am. Chem. Soc.* **2015**, *137*, 5312−5315.
(36) Kholodar, S. A.; Allen, C. L.; Gulick, A. M.; Murkin, A. S. *J. Am. Chem. Soc.* **2015**, *137*, 2748−2756.
(37) Kholodar, S. A.; Murkin, A. S. *Biochemistry* **2013**, *52*, 2302−2308.
(38) Ray, W. J., Jr.; Long, J. W.; Owens, J. D. *Biochemistry* **1976**, *15*, 4006−4017.
(39) Wolfenden, R. *Mol. Cell. Biochem.* **1974**, *3*, 207−211.
(40) Richard, J. P.; Zhai, X.; Malabanan, M. M. *Bioorg. Chem.* **2014**, *57*, 206−212.
(41) Amyes, T. L.; Richard, J. P. *Biochemistry* **2013**, *52*, 2021−2035.
(42) Malabanan, M. M.; Amyes, T. L.; Richard, J. P. *Curr. Opin. Struct. Biol.* **2010**, *20*, 702−710.
(43) Kursula, I.; Salin, M.; Sun, J.; Norledge, B. V.; Haapalainen, A. M.; Sampson, N. S.; Wierenga, R. K. *Protein Eng., Des. Sel.* **2004**, *17*, 375−382.
(44) Sampson, N. S.; Knowles, J. R. *Biochemistry* **1992**, *31*, 8482−8487.
(45) O'Donoghue, A. C.; Amyes, T. L.; Richard, J. P. *Biochemistry* **2005**, *44*, 2622−2631.
(46) O'Donoghue, A. C.; Amyes, T. L.; Richard, J. P. *Biochemistry* **2005**, *44*, 2610−2621.
(47) Go, M. K.; Amyes, T. L.; Richard, J. P. *Biochemistry* **2009**, *48*, 5769−5778.
(48) Go, M. K.; Koudelka, A.; Amyes, T. L.; Richard, J. P. *Biochemistry* **2010**, *49*, 5377−5389.
(49) Go, M. K.; Amyes, T. L.; Richard, J. P. *J. Am. Chem. Soc.* **2010**, *132*, 13525−13532.
(50) Malabanan, M. M.; Koudelka, A. P.; Amyes, T. L.; Richard, J. P. *J. Am. Chem. Soc.* **2012**, *134*, 10286−10298.
(51) Malabanan, M. M.; Amyes, T. L.; Richard, J. P. *J. Am. Chem. Soc.* **2011**, *133*, 16428−16431.
(52) Pollack, R. M. *Bioorg. Chem.* **2004**, *32*, 341−353.
(53) Schwans, J. P.; Sunden, F.; Gonzalez, A.; Tsai, Y.; Herschlag, D. *J. Am. Chem. Soc.* **2011**, *133*, 20052−20055.
(54) Kraut, D.; Sigala, P.; Fenn, T.; Herschlag, D. *Proc. Natl. Acad. Sci. U. S. A.* **2010**, *107*, 1960−1965.
(55) Bergemeyer, H. U.; Haid, E.; Nelboeck-Hochstetter, M.; Office, U. P., Ed.: US 3,662,037, 1972.
(56) Sun, J.; Sampson, N. S. *Biochemistry* **1999**, *38*, 11474−11481.
(57) Gasteiger, E.; Hoogland, C.; Gattiker, A.; Duvaud, S.; Wilkins, M. R.; Appel, R. D.; Bairoch, A. *Proteomics Protocol Handbook* **2005**, 571−607.
(58) Gasteiger, E.; Gattiker, A.; Hoogland, C.; Ivanyi, I.; Appel, R. D.; Bairoch, A. *Nucleic Acids Res.* **2003**, *31*, 3784−3788.
(59) Plaut, B.; Knowles, J. R. *Biochem. J.* **1972**, *129*, 311−320.
(60) Amyes, T. L.; Richard, J. P. *J. Am. Chem. Soc.* **1996**, *118*, 3129−3141.
(61) Amyes, T. L.; Richard, J. P. *J. Am. Chem. Soc.* **1992**, *114*, 10297−10302.
(62) Malabanan, M. M.; Go, M.; Amyes, T. L.; Richard, J. P. *Biochemistry* **2011**, *50*, 5767−5679.
(63) Trentham, D. R.; McMurray, C. H.; Pogson, C. I. *Biochem. J.* **1969**, *19*, 114.
(64) Go, M. K.; Malabanan, M. M.; Amyes, T. L.; Richard, J. P. *Biochemistry* **2010**, *49*, 7704−7708.
(65) Sampson, N. S.; Knowles, J. R. *Biochemistry* **1992**, *31*, 8488−8494.
(66) Berlow, R. B.; Igumenova, T. I.; Loria, J. P. *Biochemistry* **2007**, *46*, 6001−6010.
(67) Barnett, S. A. Ph.D. Dissertation. University at Buffalo: Buffalo, New York, 2009.
(68) Miller, B. G.; Butterfoss, G. L.; Short, S. A.; Wolfenden, R. *Biochemistry* **2001**, *40*, 6227−6232.
(69) Goryanova, B.; Goldman, L. M.; Ming, S.; Amyes, T. L.; Gerlt, J. A.; Richard, J. P. *Biochemistry* **2015**, *54*, 4555−4564.
(70) Jencks, W. P. *Chem. Rev.* **1985**, *85*, 511−527.
(71) Kirsch, J. F., Ed. *Linear Free Energy Relations in Enzymology*; Plenum Publishing Co. Ltd.: New York, 1972.
(72) Richard, J. P.; Westerfeld, J. G.; Lin, S. *Biochemistry* **1995**, *34*, 11703−11712.
(73) Richard, J. P.; Westerfeld, J. G.; Lin, S.; Beard, J. *Biochemistry* **1995**, *34*, 11713−11724.
(74) Williams, A. *Adv. Phys. Org. Chem.* **1992**, *27*, 1−55.
(75) Labow, B. I.; Herschlag, D.; Jencks, W. P. *Biochemistry* **1993**, *32*, 8737−8741.
(76) Barelier, S.; Cummings, J. A.; Rauwerdink, A. M.; Hitchcock, D. S.; Farelli, J. D.; Almo, S. C.; Raushel, F. M.; Allen, K. N.; Shoichet, B. K. *J. Am. Chem. Soc.* **2014**, *136*, 7374−7382.
(77) Jencks, W. P. *Proc. Natl. Acad. Sci. U. S. A.* **1981**, *78*, 4046−4050.
(78) Alber, T.; Banner, D. W.; Bloomer, A. C.; Petsko, G. A.; Phillips, D.; Rivers, P. S.; Wilson, I. A. *Philos. Trans. R. Soc., B* **1981**, *293*, 159−171.
(79) Kursula, I.; Wierenga, R. K. *J. Biol. Chem.* **2003**, *278*, 9544−9551.
(80) Jencks, W. P. *Cold Spring Harbor Symp. Quant. Biol.* **1987**, *52*, 65−73.
(81) Jencks, W. P. *Adv. Enzymol. Relat. Areas Mol. Biol.* **2006**, *43*, 219−410.
(82) Wang, Y.; Berlow, R. B.; Loria, J. P. *Biochemistry* **2009**, *48*, 4548−4556.
(83) Casteleijn, M. G.; Alahuhta, M.; Groebel, K.; El-Sayed, I.; Augustyns, K.; Lambeir, A. M.; Neubauer, P.; Wierenga, R. K. *Biochemistry* **2006**, *45*, 15483−15494.
(84) Goryanova, B.; Goldman, L. M.; Amyes, T. L.; Gerlt, J. A.; Richard, J. P. *Biochemistry* **2013**, *52*, 7500−7511.
(85) Zhai, X.; Go, M. K.; O'Donoghue, A. C.; Amyes, T. L.; Pegan, S. D.; Wang, Y.; Loria, J. P.; Mesecar, A. D.; Richard, J. P. *Biochemistry* **2014**, *53*, 3486−3501.
(86) Amyes, T. L.; Richard, J. P.; Tait, J. J. *J. Am. Chem. Soc.* **2005**, *127*, 15708−15709.
(87) Joseph-McCarthy, D.; Lolis, E.; Komives, E. A.; Petsko, G. A. *Biochemistry* **1994**, *33*, 2815−2823.
(88) Miller, B. G.; Hassell, A. M.; Wolfenden, R.; Milburn, M. V.; Short, S. A. *Proc. Natl. Acad. Sci. U. S. A.* **2000**, *97*, 2011−2016.
(89) Antoniou, D.; Schwartz, S. D. J. *J. Phys. Chem. B* **2011**, *115*, 15147−15158.
(90) Antoniou, D.; Basner, J.; Nunez, S.; Schwartz, S. D. *Adv. Phys. Org. Chem.* **2006**, *41*, 315−362.
(91) Mincer, J. S.; Nunez, S.; Schwartz, S. D. *J. Theor. Comput. Chem.* **2004**, *3*, 501−509.
(92) Glowacki, D. R.; Harvey, J. N.; Mulholland, A. *J. Biochem. Soc. Symp.* **2012**, *79*, 43−55.
(93) Kohen, A. *Acc. Chem. Res.* **2015**, *48*, 466−473.
(94) Joseph, D.; Petsko, G. A.; Karplus, M. *Science* **1990**, *249*, 1425−1428.
(95) Kurkcuoglu, Z.; Bakan, A.; Kocaman, D.; Bahar, I.; Doruker, P. *PLoS Comput. Biol.* **2012**, *8*, e1002705.
(96) Desamero, R.; Rozovsky, S.; Zhadin, N.; McDermott, A.; Callender, R. *Biochemistry* **2003**, *42*, 2941−2951.


DOI: 10.1021/jacs.5b09328
*J. Am. Chem. Soc.* 2015, 137, 15185−15197

(97) Rozovsky, S.; McDermott, A. E. *J. Mol. Biol.* **2001**, *310*, 259−270.
(98) Rozovsky, S.; Jogl, G.; Tong, L.; McDermott, A. E. *J. Mol. Biol.* **2001**, *310*, 271−280.
(99) Williams, J. C.; McDermott, A. E. *Biochemistry* **1995**, *34*, 8309−8319.



DOI: 10.1021/jacs.5b09328
*J. Am. Chem. Soc.* 2015, 137, 15185−15197